Principal Crystal and Molecular Paramagnetic Susceptibilities of Bis(*N*-isopropylsalicylideneiminato)nickel(II) †

By **Denis A. Cruse** and **Malcolm Gerloch,*** University Chemical Laboratories, Lensfield Road, Cambridge CB2 1EW

Principal crystal paramagnetic susceptibilities of the title complex throughout the range 20—295 K are reported. A new compact Faraday balance for the measurement of crystal magnetic properties in this temperature range is described. The experimental susceptibilities, together with the crystal transmission spectrum, have been fitted by a quantum-mechanical model in which no fictitious symmetry higher than shown in the true molecular geometry is presumed. The ligand field is parameterized by the angular-overlap model. Parameter values for σ and π bonding and for spin–orbit and orbital-reduction effects have been determined which reproduce the experimental susceptibilities to within ±2% throughout the temperature range. The calculated orientations of the principal molecular susceptibilities are compared with the co-ordination geometry of the complex.

UNTIL recently, studies of the paramagnetic susceptibilities of mononuclear transition-metal complexes have been restricted mostly to molecules suffering trigonal or tetragonal distortions from octahedral or tetrahedral geometries.[1] Often such relatively high molecular symmetries have been assumed or idealized for reasons of theoretical tractability even where the true symmetry is much lower. More important is that the consequent neglect of the majority of paramagnetic complexes, those with molecular symmetry too low to be treated within the framework of older theoretical models, constitutes a gross loss of potential information in magnetochemistry. This situation is changed entirely by the advent of a recent theoretical model allowing calculation of the magnetic properties of mononuclear complexes of any geometry.[2]

The ligand field is parameterized within this model by the angular-overlap framework of Schäffer and Jørgensen.[3-5] A central feature of our exploitation of this model must be to establish a catalogue of angular-

---

† No reprints available.

[1] M. Gerloch, *M.T.P. Internat. Rev. Sci., Phys. Chem., Ser* 2, 1976, **2**, 195.

[2] M. Gerloch and R. F. McMeeking, *J.C.S. Dalton*, 1975, 2443.

[3] C. E. Schäffer and C. K. Jørgensen, *J. Inorg. Nuclear Chem.*, 1958, **8**, 143.

[4] C. E. Schäffer and C. K. Jørgensen, *Mat. Fys. Medd. Kgl. Dan. Vid Selsk*, 1965, **34**, 13.

[5] C. E. Schäffer, *Structure and Bonding*, 1968, **5**, 68.

overlap parameters with respect to metal and ligand donor groups analogous to the spectrochemical series, in the hope that they may be transferable from system to system and that they may correlate with bonding features established by other means. Two studies along these lines have been published recently.[6,7] The work described here extends this approach to a nickel(II) complex in which the metal atom is co-ordinated by two Schiff-base ligands in a formally tetrahedral geometry. So many transition-metal complexes have been prepared with Schiff bases that a detailed study of the magnetic properties, with full recognition of the very low molecular symmetry actually obtained, hopefully provides a searching and fairly general test of the techniques.

Bis(*N*-isopropylsalicylideneiminato)nickel(II), (1), has been the subject of an earlier susceptibility study,[8] which was characterized by the simplifying assumption of an

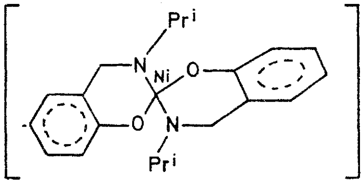

(1)

axial distortion from tetrahedral symmetry (D_{2d}) together with the difficult choice of directions for the principal magnetic susceptibilities $K_{\parallel}$ and $K_{\perp}$. After fitting experimental powder susceptibilities and magnetic anisotropies, measured by the Gouy and Krishnan techniques in the range 90—300 K, very low values for the orbital-reduction factor k and of the spin–orbit coupling coefficient ζ (—*ca.* 0.4 and 200 cm^{-1}, respectively) were deduced. While this represented the best compromise to be achieved with the experimental and theoretical resources then available, the present work is designed to improve the position in all respects.

On the experimental side we have measured the principal crystal susceptibilities directly throughout the range 20—300 K and we describe a new Faraday balance which makes such measurements routine. On the theoretical side we hoped to consider the following specific points: (*i*) how well and how uniquely is the new, more rigorous, theoretical model able to fit the experimental data, especially over the extended temperature range now available; (*ii*) how well do best-fit angular-overlap π-bonding parameters for the imine and phenolic oxygen donors compare with chemical experience and contrast with those found [6,7] for pyridine, thiocyanate, halogens, and pentane-2,4-dione complexes of Fe^{II} and Co^{II}; (*iii*) how dependent on the restricted nature of the earlier model [8] are the low values for the k and ζ parameters; and (*iv*) where do the principal molecular susceptibilities lie in relation to various features of the co-ordination shell and how serious was the early idealized presumption of D_{2d} symmetry.

EXPERIMENTAL

Faraday Balance.—Our design of the apparatus was guided by two main requirements. We wished to measure the magnetic susceptibilities of small samples as powders and, especially, as single crystals. In the latter case we prefer to determine principal susceptibilities directly rather than rely on the intrinsically less accurate measurements of magnetic anisotropies. Secondly, we wanted to cover a large temperature range but with a minimum of cryogenic techniques so that procedures may be as routine as possible. These criteria are satisfied by the apparatus shown schematically in Figure 1.

Susceptibilities were measured by the Faraday technique using a special sample-suspension device and a rotating magnet. Cooling was achieved with the consumption of electrical power but with no cryogens, using a commercial closed-cycle helium-gas heat pump. The 'Cryocooler' (Cryogenic Technology Incorporated) was attached directly to the sample chamber between the magnet poles and held in a simple cradle which rotated with the magnet.

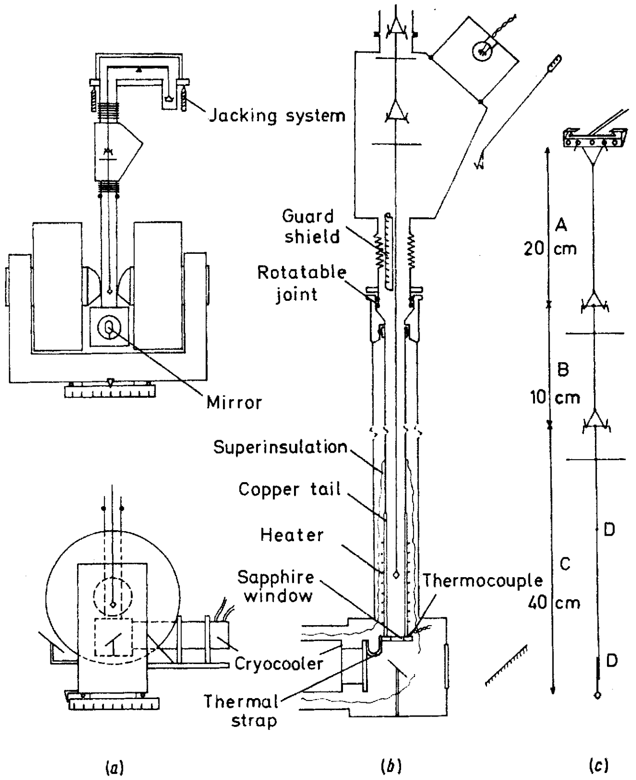

FIGURE 1 Faraday balance showing (*a*) overall views of the rotating sub-assembly, (*b*) the cryostat and sample-loading box, and (*c*) the sample suspension. The drawings are schematic only and not to scale

The cryostat (Oxford Instruments) is shown in detail in Figure 1(*b*). The sample chamber comprised a stainless-steel tube (*ca.* 8 mm in diameter) having a copper tail and a sapphire window at the base for inspection of the sample *via* a simple mirror system. Cooling was achieved through the thick copper strap connecting the Cryocooler and sample tube, heating by means of a nichrome coil around the copper

---

[6] M. Gerloch, R. F. McMeeking, and A. M. White, *J.C.S. Dalton*, 1975, 2452.

[7] M. Gerloch, R. F. McMeeking, and A. M. White, *J.C.S. Dalton*, 1976, 655.

[8] M. Gerloch and R. C. Slade, *J. Chem. Soc.* (*A*), 1969, 1022.

tailpiece. A gold–iron (0.03% Fe)–chromel thermocouple, soldered with Wood's metal to the copper flange at the base of the sample tube, served for temperature measurement and control. An external liquid-nitrogen reference junction completed the thermocouple. Temperature control was effected by a Precision Temperature Controller (Oxford Instruments).

Samples were weighed by an electromicrobalance (Sartorious, model 4433) accurate to 0.1 μg, supported on a commercial jacking system (Oxford Instruments) with an additional facility for two-dimensional lateral adjustment. Samples could thus be centred in the sample tube and moved vertically in a reproducible fashion. The cryostat, cooler, and magnet rotated together with respect to the microbalance and jacking system which were fixed. This is made possible by a simple rotating joint with O rings as illustrated in Figure 1(*b*). The diagram also shows the adapter for sample loading (Oxford Instruments). A semi-cylindrical metal sleeve, loose-fitting inside the connecting bellows, prevented samples being caught up in the bellow folds on being raised and lowered in the cryostat. The magnet had special Faraday-profile pole tips, 10 cm in diameter with an adjustable gap (*ca.* 3 cm here): these and the power supply were from Bruker Spectrospin.

The remaining feature, shown in Figure 1(*c*), is our suspension system designed to be light, to permit easy sample loading, and to prevent rotation of the sample so that susceptibilities may be measured as functions of crystal orientation simply by rotation of the magnet sub-assembly. The maximum balance loading permissible was 3.0 g: the suspension shown in Figure 1(*d*) weighed somewhat less than 1 g. Only the lowest section (C) was removed when changing samples, the cross-piece serving both as a ' lifting handle ' and as a guard against the whole section falling into the cryostat in case of accident. The vertical components of this section were made of quartz, by virtue of its low coefficient of expansion, poor thermal conductivity, and lack of paramagnetism. Two joins (D) were made with ' Durofix ' for ease of replacement (sample change or breakage), the rest with Araldite epoxy resin. The whole suspension was in three parts merely for ease of dismantling the superstructure. The overall length of *ca.* 70 cm ensures that the microbalance is completely unaffected by the magnetic field. We observed no sample rotation with this device as the magnet was rotated, even with very anisotropic paramagnetic crystals: also balance readings were reproducible when a given magnet orientation was approached from either direction. The suspension is light, flexible (necessary for sample loading) and, with reasonable care, robust.

Weighed crystals were accurately oriented by *X*-ray techniques with a chosen axis parallel to the goniometer axis. The crystal was then transferred, in identical orientation, from the arcs to a short length (*ca.* 3 cm) of quartz fibre, with Durofix as adhesive, using a special jig. Thus mounted, the sample and fibre were subsequently attached (Durofix) to the end of the lowest section (C) of the suspension ready for measurement.

Running Conditions.—(a) *Field profile.* We found that lateral adjustment of the crystal within the sample chamber, *i.e.* ±3 mm, produced no significant change in force. Vertical adjustment by ±0.5 cm from the position of maximum force introduced a force change of *ca.* 2%. Vertical setting was easily achieved within ±0.01 cm. The crystals measured had maximum dimensions of *ca.* 5 mm, and the maximum difference in force between the extremities and middle of such a crystal was less than 0.5%. As a matter of routine, the position of maximum force was established at the beginnning of each run, including calibration runs.

(b) *Helium environment.* Commercial grade helium gas had sufficient impurities to cause noticeable (by weight and appearance) condensation on the sample at low temperatures. Accordingly, we used helium gas, passed slowly (using a glass frit) through a column of molecular sieves (grade 5A) immersed in liquid nitrogen.* The column was *ca.* 1 m long, 2 cm in diameter, in the form of a series of U tubes. The sample chamber and electrobalance were evacuated and refilled four times with the helium so purified. The sieves were regenerated every 4—5 runs by baking to 10^{-3} Torr † at *ca.* 240 °C for several hours.* Difficulties in making the sample chamber, loading box, and balance sufficiently vacuum tight to prevent ingress of air and subsequent condensation on cold samples under conditions of low helium-gas pressures (as is common practice) were overcome by running at *ca.* 3 lbf in^{-2} overpressure. As so little volume actually became cold, an overpressure was found to be maintained throughout the temperature range. No problems with condensation occurred under these conditions, no off-field weight drift with time, nor any time dependence of the force.

Cooldown time was *ca.* 1.25 h (compared with 0.75 h for the Cryocooler without load). The base temperature was *ca.* 20 K (compared to *ca.* 9 K without load). Temperature stabilization was better than ±0.2 K. Temperature increases below 50 K were virtually instantaneous, but required 5—10 min near room temperature: these observations derived from monitoring both the precision temperature controller and microbalance readings. Experience showed that the easier and faster experimental routine is to take readings on warming from base temperature. A typical run of 20 temperatures for two magnet orientations required 6 h. Overall, the procedures are reliable, repeatable, and routine.

Calibration.—The sample was suspended in helium gas, an excellent heat conductor, within the copper tail section of the sample tube. However, there was a large temperature gradient from the base of the tube, which is coupled directly to the cryocooler at 9 K, to the top of the tube at room temperature. The thermocouple, mounted on the outside of the copper flange at the base of the sample tube, cannot therefore be relied on to measure sample temperatures directly. Accordingly we calibrated the thermocouple *in situ* against the known temperature dependence of the susceptibility[9] of manganese(II) Tutton Salt, $\text{Mn[SO}_4\text{]}\cdot\text{[NH}_4\text{]}_2\text{[SO}_4\text{]}\cdot 6\text{H}_2\text{O}$. Crystals of this salt do not effloresce in dry helium gas, are virtually magnetically isotropic, and exhibit Curie–Weiss behaviour for their susceptibility (Weiss constant, $\theta = 0.0$ K) down to *ca.* 1 K. The procedure was repeated for several crystals with masses ranging from 1 to 5 mg. At room temperature the reading of the precision temperature controller (*i.e.* the temperature of the thermocouple) differed from the true temperature (of the sample) by *ca.* 10°.

This calibration routine simultaneously furnishes an

---

* We thank Miss M. Laffey and Dr. P. Thornton of Queen Mary College, London, for their advice on these procedures.

† Throughout this paper: 1 Torr = (101 325/760) Pa; 1 lbf $\text{in}^{-2} \approx (9.8 \times 4\,536)/6.45$ Pa.

[9] E. König, ' Tables of Magnetic Susceptibilities,' Landolt-Börnstein, eds. K. H. Hellwege and A. M. Hellwege, 1965, Springer–Verlag, Berlin.

absolute calibration of the complete instrument, relating force and susceptiblity for a given field strength. The process was repeated for various magnet coil currents. Wolf[10] commented on the unreliability of calibrating a Faraday balance with isotropic materials in this way if anisotropic crystals are to be measured subsequently. We found, however, no doubt as a result of improved magnet pole-piece design, that no significant error arose from cross-fields: good agreement was found with principal susceptibilities of various crystals measured by us and by others using the Krishnan and other techniques.

In the calibration and all the subsequent runs the diamagnetic correction for the suspension was determined by removing the crystal and replacing the small amount of Durofix removed with it. Further experiments showed that the amount of adhesive used for different runs varies little, as does the associated diamagnetic correction, thus lending further reliability to this technique.

RESULTS

Crystals of bis(*N*-isopropylsalicylideneiminato)nickel(II), (1), kindly given by Dr. R. C. Slade, were prepared by the literature method[11] and gave satisfactory C, N, and H analyses. The dark green crystals are orthorhombic[11] and measurements were made on samples weighing *ca.* 3 mg. Crystals were oriented in two ways: with *a* and *c* parallel to the suspension. Measurements thus gave values for χ_b and χ_c by suitable rotation of the magnet, for the first mounting, and for χ_b and χ_a for the second. The separately determined values of χ_b common to the two mountings agreed within $\pm 1\%$ throughout the temperature range and are averaged in Table 1 which presents interpolated results for all the three principal susceptibilities in the range 20—295 K. Results at >90 K agree within 1% with those reported earlier, measured by the Krishnan technique. No field dependence of susceptibilities ($B \leqslant 1T$) was noted at low temperatures. The results in Table 1 illustrate the much greater temperature variation of magnetic moments which occurs below the liquid-nitrogen range. This behaviour obviously poses a more exacting test for the theoretical model than the data from the more restricted liquid-nitrogen cryostat range.

TABLE 1

Experimental crystal susceptibilities (10^{-6} c.g.s.units) and average moments of complex (1)

T/K	χ_a	χ_b	χ_c	$\bar{\chi}$	$\bar{\mu}$
295	3 960	4 920	4 380	4 420	3.23
285	4 090	5 080	4 520	4 560	3.23
275	4 220	5 250	4 670	4 710	3.22
265	4 370	5 440	4 830	4 880	3.22
255	4 520	5 640	5 070	5 060	3.21
245	4 690	5 870	5 210	5 260	3.21
235	4 880	6 110	5 420	5 470	3.21
225	5 080	6 370	5 650	5 700	3.20
215	5 280	6 660	5 900	5 950	3.20
205	5 510	6 990	6 180	6 220	3.19
195	5 780	7 360	6 490	6 550	3.19
185	6 070	7 770	6 840	6 890	3.19
175	6 360	8 200	7 200	7 250	3.19
165	6 690	8 680	7 610	7 660	3.18
155	7 060	9 210	8 060	8 110	3.17
145	7 480	9 830	8 580	8 630	3.16
135	7 980	10 600	9 200	9 250	3.16
125	8 560	11 400	9 930	9 970	3.16
115	9 210	12 400	10 700	10 800	3.15
105	9 930	13 600	11 600	11 700	3.14
95	10 800	15 700	12 800	12 900	3.13
85	11 800	16 900	14 200	14 300	3.11
75	13 000	19 100	15 900	16 000	3.10
65	14 400	21 800	17 900	18 000	3.06
55	16 000	25 400	20 400	20 600	3.01
45	17 900	29 700	23 500	23 700	2.92
35	19 500	34 800	26 900	27 100	2.75
25	20 800	40 400	30 200	30 400	2.47
20	21 100	42 500	31 300	31 600	2.25

DISCUSSION

We fitted the experimental results by the general theoretical model for susceptibilities described earlier.[2] Calculations were made within the complete spin-triplet basis ($^3F + {}^3P$) free-ion terms. The parameter set comprised B, ζ, and k for interelectron repulsion, spin–orbit coupling, and orbital-reduction effects, together with angular-overlap parameters as follows. Sigma bonding from the phenolic oxygen atoms and from the imine nitrogens is represented by $e_\sigma(\mathrm{O})$ and $e_\sigma(\mathrm{N})$. Normal to these directions, orientations for π bonding from these donor atoms are defined in (y), and perpendicular to (x), the Schiff-base planes. The C=N bond order was assumed to be two, as evidenced by the crystallographic[11] bond length of 1.30 Å, and the σ bonding associated with the imine nitrogen atom was taken as sp^2 hybridized. Accordingly, we assumed that π bonding between nitrogen and metal in the plane of the sp^2 hybrids is negligible, *i.e.* $e_{\pi y}(\mathrm{N}) = 0$. This assumption is justified later. The bond orders associated with the phenolic oxygen are less clear but certainly not well described as double. In order to avoid prejudging the situation here, we include both $e_{\pi x}(\mathrm{O})$ and $e_{\pi y}(\mathrm{O})$ as parameters to be fitted by experiment. Altogether, therefore, the ligand field is parameterized by $e_\sigma(\mathrm{O})$, $e_\sigma(\mathrm{N})$, $e_{\pi x}(\mathrm{N})$, $e_{\pi x}(\mathrm{O})$, and $e_{\pi y}(\mathrm{O})$.

In view of the impracticality of wide and simultaneous variation of all the parameters in these lengthy computations, we adopted a strategy for fitting theory to experiment similar to that pursued in earlier work.[6,7] Thus we chose values from the literature, and with prejudice, for those parameters likely to determine the electronic spectrum more than the magnetic moments, namely B and e_σ, and varied e_π for best fit. Such values only represent a starting point for the fitting procedure, however, and were themselves varied after some knowledge was gained of the e_π parameters. From the earlier study of this complex, we took $B = 800$ cm^{-1}, a value only approximately derived from fitting to a tetrahedral model for the chromophore. For simplicity, we took $e_\sigma(\mathrm{O}) = e_\sigma(\mathrm{N})$ initially. By comparison with such values[6] in $[\mathrm{Co(py)_4(NCS)_2}]$ and $[\mathrm{Fe(py)_4(NCS)_2}]$ (py = pyridine), we might expect $3\,000 < e_\sigma < 4\,000$ cm^{-1}. Further, fitting to a tetrahedral model in the earlier study suggested $\Delta_{\mathrm{tet}} \sim 3\,700$ and since $\Delta_{\mathrm{tet}} = -(4/9)(3e_\sigma - 4e_\pi)$ and the most naïve overlap models suggest[1] $e_\pi \sim 0.25e_\sigma$, we deduce $e_\sigma \sim 4\,200$ cm^{-1}. Both estimates are very approximate, of course: for our starting set of parameters we took $e_\sigma = 3\,500$ cm^{-1} for both oxygen and nitrogen donors. The value for the spin–orbit coupling coefficient deduced from the earlier study was *ca.* 200

---

[10] W. P. Wolf, *J. Appl. Phys.*, 1957, **28**, 780.

[11] M. R. Fox, P. L. Orioli, E. C. Lingafelter, and L. Sacconi, *Acta Cryst.*, 1964, **17**, 1159.

cm^{-1}, while that for the $[NiCl_4]^{2-}$ ion reported[8] at the same time was *ca.* 350 cm^{-1}. The free-ion value is $\zeta_0 = 630$ cm^{-1}, so that the value of 200 cm^{-1} seems surprisingly low and we began, therefore, by taking the higher value $\zeta = 350$ cm^{-1}.

With values of B, $e_\sigma(O)$, $e_\sigma(N)$, and ζ so fixed, we next calculated susceptibilities for values of $e_\pi(N)$, $e_{\pi x}(O)$, and $e_{\pi y}(O)$ varying in steps of 200 cm^{-1} in the range 0—1 600 cm^{-1} and for the orbital-reduction factor k varying from 1.0 to 0.2 in steps of 0.2. Calculated values for all the three principal crystal susceptibilities throughout the range 20—295 K were compared with the experimental results listed in Table 1, using the mapping procedures described earlier.[6] The result was a single region of the four-dimensional parameter space (three e_π values + k) in which fits were excellent. The region was approximately 'spherical' in this space and centred on the values $e_{\pi x}(N) = 800$ cm^{-1}, $e_{\pi x}(O) = 600$ cm^{-1}, $e_{\pi y}(O) = 800$ cm^{-1}, and $k = 0.4$.

With these π-parameter values fixed and the same values for $e_\sigma(O) = e_\sigma(N)$, a new three-dimensional fitting region was explored in which ζ ranged from 150 to 650 cm^{-1}, in steps of 100 cm^{-1}, B ranged from 500 to 1 100 ($\times$ 100) cm^{-1}, and k 0.4—0.6 in steps of 0.05. A single fitting region in polyparameter space was again found, best fits being fairly sensitive to ζ (by ± 50 cm^{-1}) but rather insensitive to B. The original choices of $\zeta = 350$ cm^{-1} and $B = 800$ cm^{-1} actually corresponded to the values for best fit, a result not wholly serendipitous.

Now with e_π and B values fixed, fits were investigated for simultaneous variation of ζ ranging from 325 to 425 cm^{-1} ($\times 25$ cm^{-1}) and $e_\sigma(O) \neq e_\sigma(N)$ ranging from 2 500 to 4 500 cm^{-1} in 500 cm^{-1} steps. The region of good fit was again single but showed a degree of correlation between e_σ, ζ, and k values. The region was effectively bounded by $3\,000 < e_\sigma < 4\,200$ cm^{-1} with $e_\sigma(O)$ equal to, or perhaps slightly larger than, $e_\sigma(N)$. As e_σ varied from 3 000 to 4 000 cm^{-1}, the best fits required ζ to change from 325 to 375 cm^{-1} respectively and, at the same time, k to vary from 0.45 to 0.55. Fits throughout this region were all good.

TABLE 2

Parameter values (in cm^{-1}, except k) for the best fits to magnetic susceptibilities ($B = 800$ or 750 cm^{-1})

Sample fit	$e_\sigma(O) =$ $e_\sigma(N)$	ζ	$e_{\pi x}(N)$	$e_{\pi x}(O)$	$e_{\pi y}(O)$	k
A	3 000	325	700	400	600	0.45
B	3 500	350	800	600	800	0.45
C	4 000	375	900	700	1 000	0.50

Refinement was continued by calculating susceptibilities with B fixed at 800 cm^{-1} and for each of $e_\sigma(O) = e_\sigma(N) = 3\,000$, 3 500, and 4 000 cm^{-1} with correlated ζ values of 325, 350, and 375 cm^{-1}, respectively, allowing variation in e_π parameters once more. With $e_\pi(N)$ ranging from 600 to 1 000 ($\times 100$) cm^{-1}, we now found a degree of correlation between the π parameters and the rest. The situation is summarized in Table 2 and is found to be insensitive to change in B of ± 50 cm^{-1}.

Finally, the initial presumption that $e_{\pi y}(N) = 0$ was checked by calculations with the other parameters taking the values in Table 2 but with $e_{\pi y}(N)$ being free to vary from 0 to 1 000 cm^{-1}. The fit between calculated and observed susceptibilities was markedly impaired as $e_{\pi y}(N)$ deviated from zero: even a change of 200 cm^{-1} worsened the fit from *ca.* 2 to *ca.* 6%.

Comparison with the Optical Spectrum.—Eigenvalues calculated prior to the magnetic field perturbation may be compared with the electronic spectrum reported earlier.[8] These are displayed graphically in Figure 2 for the fits in Table 2 and compared with the spectral trace. For simplicity, components of a formal spin triplet (actually split by spin–orbit coupling and the low-symmetry field) are shown as thick bars. The energy levels shown in the Figure correspond to the parameter values in Table 2 with $B = 750$ cm^{-1}, a value which improved fitting of components from $^3T_1(T_d)$ to the spectrum without undue adverse effects on the calculated susceptibilities. We note that fit C gives best agreement with the spectrum by predicting the level arising from $^3A_2(T_d)$ at *ca.* 9 000 cm^{-1}. Although this is observed as a weak band, parameters for fits A and B (in the middle and far end of the susceptibility fitting region) are unable to reproduce this feature of the spectrum correctly. We do not consider the quality of this spectrum, although from a single crystal at 80 K, to be sufficient to use as a basis for refinement of the ligand-field parameters. There does, however, appear to be sufficient evidence from the spectrum to favour a magnetic fit corresponding to fit C in Table 2. Furthermore, the larger value of e_σ this implies agrees well with the estimate made at the outset of the fitting procedure, although such agreement is not to be relied on by itself. The fitting procedure was concluded by visual interpolation of the fitting maps to yield the final set of parameter values:

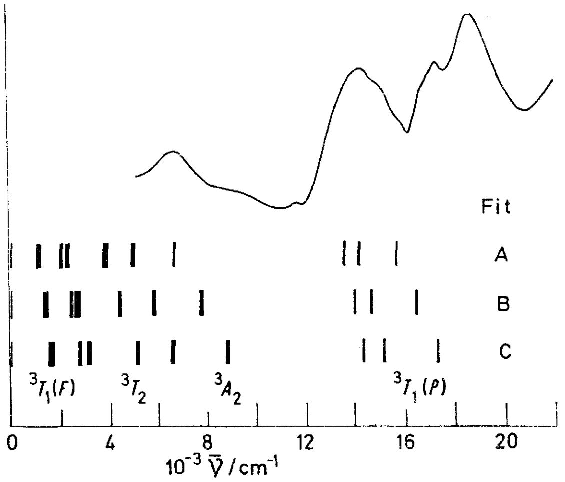

FIGURE 2 Comparison between the crystal transmission spectrum (ref. 8) and eigenvalues of (1) corresponding to the susceptibility fits in Table 2. Bar thicknesses denote the energy spread of components of the spin triplets

$$B = 750 \text{ cm}^{-1},\ e_\sigma(N) = 3\,800 \text{ cm}^{-1},\ e_\sigma(O) = 4\,200 \text{ cm}^{-1},$$
$$\zeta = 375 \text{ cm}^{-1},\ k = 0.5,\ e_\pi(N) = 930 \text{ cm}^{-1},$$
$$e_{\pi x}(O) = 660 \text{ cm}^{-1},\ e_{\pi y}(O) = 1\,000 \text{ cm}^{-1}.$$

The excellent agreement between crystal susceptibilities calculated with this set of values and experimental values from Table 1 is shown in Figure 3.

Conclusions.—The problems posed in the introduction are now discussed in the light of the results just described.

(*i*) The quantum-mechanical model is seen to fit the magnetic and spectral data remarkably well, in particular the absolute values and temperature dependences of all the three principal susceptibilities throughout the whole range 20—295 K. While the earlier D_{2d} model [8] involved parameterization of the geometry by θ, the angle representing distortion of donor bond angles from the approximate inversion tetrad, the present formalism presumes the exact co-ordination geometry explicitly. All the ligand-field parameters are thus radial parameters, directly relating to the various bonding modes of each donor atom. Despite the more rigorous requirements of the low-symmetry model, fits are remarkably unique in that only one region of polyparameter space describes good agreement between theory and experiment. Within this region there is a spread of satisfactory parameters, but with a degree of correlation between them. Most important, however, is that there are no other separate regions of fit. Furthermore, comparison with spectral data strongly suggests a sharpening of the fitting region as detailed above.

(*ii*) The e_σ parameters for best fit to magnetism and spectra indicate approximately equal magnitudes for σ bonding from the phenolic oxygen and imine nitrogen donor atoms; there is some indication that the oxygen is a slightly better σ donor but, if so, by a few percent only. The e_σ values are a little greater than those for pyridine in $[Co(py)_4(NCS)_2]$ and $[Fe(py)_4(NCS)_2]$ but the values in these latter complexes were probably less well defined by the experiments.[6]

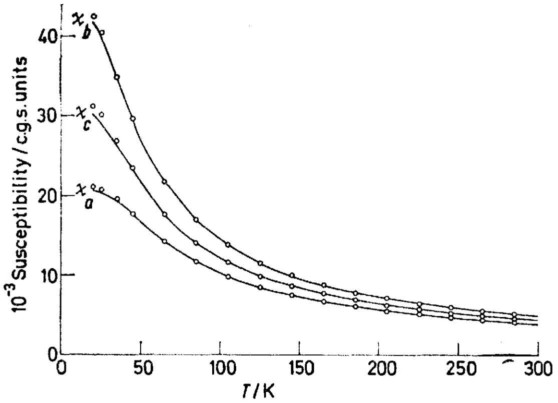

FIGURE 3 Comparison between observed (circles) and calculated crystal susceptibilities of (1) for final parameter values given

The π-bonding parameters in the present case are much greater than for pyridine ligands, however. For the imine nitrogen-donor atom, the value $e_\pi = 930$ cm^{-1} {compared with *ca.* 100 cm^{-1} for pyridine in $[M(py)_4(NCS)_2]$ (M = Co or Fe)} tends towards a value to be expected from $e_\pi/e_\sigma = 0.25$ based on the ratio of σ and π overlap integrals of pure p wavefunctions on the ligands.[12] While this theoretical ratio need not obtain in practice because of the dissimilarity of the σ- and π-donor orbitals on any particular ligand, the relative values of e_σ and e_π for the imine group seem entirely compatible with a formal description of the nitrogen atom as sp^2 hybridized.

The situation with the π-bonding parameters for the phenolic oxygen donor is much less clear. Empirically, we find comparable degrees of π bonding associated with directions in, and perpendicular to, the aromatic ring, actually *ca.* 30% larger in the ring plane. Further the e_π(O) parameters are of the same order of magnitude as e_π(N), so we may describe the π-donor abilities of the two donor groups as similar, but for the fact that the imine group π-bonds in one direction only. We also observe an order-of-magnitude similarity between the π-bonding parameters for this phenolic oxygen donor and the ketonic oxygen donors [7] in $[Co(pd)_2(py)_2]$ (pd = pentane-2,4-dionate). However, in the latter case, π bonding perpendicular to the pd plane was greater, with respect to the metal atom, than in the plane: this appeared reasonable in view of the π delocalization to be expected in that system. Using similar arguments in the case of the phenolic oxygen of the present Schiff-base complex, however, it is not obvious why there should be a significant, and indeed greater, degree of π donation in the plane of the aromatic ring than perpendicular to it. Undoubtedly, the explanation lies in the nature of an approximation made in our treatment [2] of the angular-overlap model. A usual feature of this model, and one followed here, is to presume a diagonal nature for the bonding in the local M–L frame. Thus, we assume ligand σ bonds interact with metal σ bonds, π with π, but not π with σ. This is necessarily the case, of course, if such symmetry descriptions are rigorously valid. When they are not, as may be the case for what Schäffer [5] calls 'misdirected' valency, cross 'σ–π' interaction may be involved. In such cases, extra terms in the equivalent crystal-field spherical-harmonic expansion will occur, together with the necessity for extra angular-overlap parameters ('e_{cross}'). We have chosen to neglect these complications in the interests of avoiding too large a number of parameters. However, it must be pointed out that their neglect will not be satisfactorily compensated for by some sort of vectorial resolution of the 'misdirected' M–O (lone pair sp^2 hybrid) into pure σ and π components. On the other hand, some degree of scrambling between the e_σ(O) and $e_{\pi y}$(O) parameters will result. A small increase in e_σ from e_π is unlikely to be recognized, but the reverse situation of a contribution of a small part of the large e_σ to $e_{\pi y}$ might well be significant. For the moment, we consider it best to take the empirical findings for the phenolic oxygen, reserving any possible fuller treatment of this complex situation until such time as a larger body of empirical evidence, from many systems, compels further study.

(*iii*) The low value of the orbital-reduction factor k $\sim$0.50 found in the present study agrees quite well with that found [8] from the earlier model with idealized D_{2d}

---

[12] M. A. Hitchman, *J.C.S. Faraday II*, 1972, 846.

symmetry: thus there appears to be a large reduction of orbital angular momentum in this nominally tetrahedral complex, no doubt indicative of a degree of metal *d–p* mixing *via* covalency as discussed earlier.[13] However, the spin–orbit coupling coefficient ζ is not as small as found previously. The present value of 375 cm^{-1} (*cf.* 200 cm^{-1} *from* the earlier, less rigorous, study) compares well with the value of 380 cm^{-1} found [8] for $[NiCl_4]^{2-}$: the latter figure is the more reliable from the earlier study, corresponding to the higher temperature range in which the strict D_{2d} symmetry is known to be appropriate.

The value of ζ is low, corresponding to a 40% reduction from the free-ion value, $\zeta_0 = 630$ cm^{-1}. In this respect, there is also a clear comparison to be made with the reduction in k from unity, in that a first approximation to the spin–orbit coupling operator is to write $\zeta_0.kl.s$ rather than $\zeta_0.l.s$, as discussed elsewhere.[13] That k is found to be proportionately reduced more than ζ should occasion no concern when we remember that k enters into the calculations predominantly for the ground states, while ζ is involved rather more than k in the various admixed excited states for which different k values may be appropriate. A further difference in detail between the present and earlier studies of this nickel complex is the assumption here of isotropic k and ζ values in the interest of minimal parameterization and, so far as ζ is concerned, in common with the usual practice of presuming spherical natures for spin–orbit and interelectron-repulsion operators.

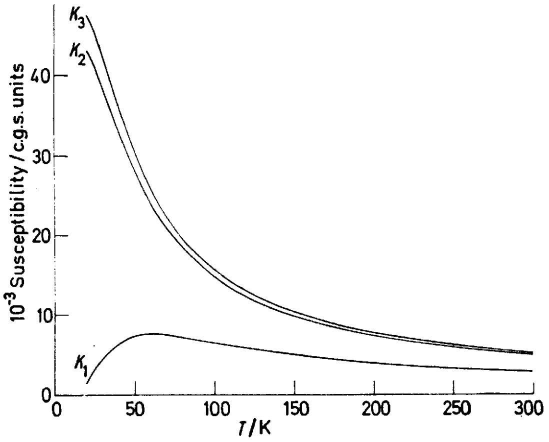

FIGURE 4 Calculated principal molecular susceptibilities of (1) for final parameter values given

(*iv*) In Figure 3 are shown the comparisons of observed and calculated principal crystal susceptibilities corresponding to the parameter values for best fit. Calculated molecular susceptibilities and moments corresponding to this fit are shown in Figure 4 and Table 3. Perhaps the most immediately obvious feature of these results is the near-axial nature of the molecular-susceptibility ellipsoid. A description in terms of $K_1 = K_{\parallel}$ and (1/2) $(K_2 + K_3) = K_{\perp}$ would be a fair approximation and it is interesting to discover the directions of the principal susceptibilities relative to the metal co-ordination shell. We note, first, that the calculated orientation of the molecular-susceptibility ellipsoid varies negligibly with respect to temperature (or k value), the maximum change being of the order of 0.5°. With respect to the orthorhombic crystal axes, the calculated molecular susceptibilities are oriented as follows:

TABLE 3

Calculated molecular susceptibilities (10^{-6} c.g.s.units) and moments of (1); final parameter values

T/K	K_1	K_2	K_3	μ_1	μ_2	μ_3
295	2 930	5 050	5 240	2.63	3.45	3.51
275	3 110	5 410	5 610	2.62	3.45	3.51
255	3 320	5 830	6 050	2.60	3.45	3.51
235	3 560	6 320	6 560	2.59	3.45	3.51
215	3 830	6 900	7 170	2.56	3.44	3.51
195	4 140	7 600	7 920	2.54	3.44	3.51
175	4 500	8 480	8 840	2.51	3.44	3.52
155	4 930	9 570	10 000	2.47	3.45	3.52
135	5 430	11 000	11 500	2.42	3.45	3.53
115	6 010	12 900	13 600	2.35	3.45	3.53
105	6 330	14 100	14 900	2.31	3.45	3.54
95	6 660	15 600	16 500	2.25	3.45	3.54
85	6 990	17 400	18 400	2.18	3.44	3.54
75	7 280	19 600	20 900	2.09	3.43	3.54
65	7 480	22 400	23 900	1.97	3.41	3.53
55	7 450	25 900	27 800	1.81	3.37	3.50
45	6 960	30 300	32 800	1.58	3.30	3.43
35	5 630	35 500	38 800	1.26	3.15	3.30
25	3 160	40 800	45 000	0.79	2.86	3.00
20	1 700	42 800	47 400	0.52	2.62	2.75

	a	b	c
K_1/°	137.9	68.8	55.6
K_2/°	52.7	90.0	37.3
K_3/°	106.8	158.8	77.3

These calculated angles are insensitive (±1°) throughout the fitting ranges of Table 2. Let us define three directions B^1, B^2, and B^3 as the bisectors of the angles O^1–Ni–N^2, O^1–Ni–O^2, and O^1–Ni–N^1, respectively (see Figure 5). The angles subtended by the principal calculated molecular susceptibilities and these bisectors are:

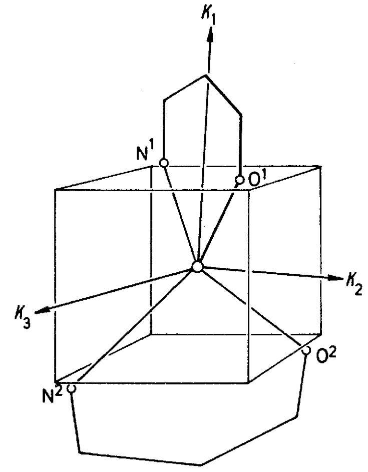

FIGURE 5 Orientation of calculated principal molecular susceptibilities of (1) with respect to the co-ordination shell

	K_1	K_2	K_3
B^1/°	84.2	74.2	14.9
B^2/°	85.0	15.6	77.2
B^3/°	8.1	88.2	83.1

---

[13] M. Gerloch and J. R. Miller, *Progr. Inorg. Chem.*, 1968, **10**, 1.

That is, the smallest susceptibility K_1, which might be approximated as $K_{\|}$, lies in a direction only 8° from the bisector of the smallest angles in the metal co-ordination shell. The other two, K_2 and K_3 of similar magnitude, lie only 15° from the other bisectors, *i.e.* close to the C_2 axes of an idealized tetrahedron (Figure 5). In our earlier work [8] on this molecule we idealized the geometry as of D_{2d} symmetry with $K_{\|}$ lying parallel to the bisector of the smaller 'intrachelate' angles (O^1–Ni–N^1 and O^2–Ni–N^2). The present work shows that those earlier assumptions were actually very good! This result need not have emerged at the outset, when we recall the low true symmetry of this molecule (C_1) and the corresponding results [6] for $[M(py)_4(NCS)_2]$ (M = Fe^{II} or Co^{II}) in which the principal molecular susceptibilities were found to lie in no obvious orientation with respect to the co-ordination geometry. Nor is the result necessarily obvious in retrospect, in view of the rather different π-bonding characteristics of the two ends of the chelate groups, *i.e.* N π-bonds in one direction only, O in two. Nevertheless, a description of the molecular magnetic property in terms of a D_{2d} approximation with $K_{\|} < K_{\perp}$ seems fair. The low value of K_1 at low temperatures is entirely compatible with the calculated ground-term splitting in which we find the formal ${}^3A_2(D_{2d})$ term gives rise to three levels at relative energies of 0, 59, and 64 cm^{-1}. Nominally, the ground states may be described as $|m_s = 0\rangle$ with $|m_s = \pm 1\rangle$ lying some 62 cm^{-1} above and split by 5 cm^{-1}.

We thank the S.R.C. for a research studentship (to D. A. C.) and for support in constructing the Faraday balance.

[6/942 *Received*, 17*th May*, 1976]